العددِ 20 شباط 2026
No.20 Feb.2026
المجلة العراقية للبحوث الانسانية والاجتماعية والعلمية
Iraqi Journal of Humanitarian, Social and Scientific Research
Print ISSN 2710-0952 Electronic ISSN2790-1254

Effect of Zinc Oxide Nanoparticles on Biofilm Formation of Escherichia coli and Klebsiella pneumoniae in Urinary Tract Infections

Aminah K Ibrahim [1]*, Ahmed Turki[1] , A.S. Obaid [2,3] *

[1] University of Anbar, College of Science, Biology Department, Ramadi, Iraq

[2] University of Anbar, College of Science, Department of Physics, Ramadi, Iraq

[3] University of Anbar, Nanomaterials Research Center, Ramadi, Iraq.

***Corresponding author: Aminah Kh. Ibrahim**
ame23s1011@uoanbar.edu.iq

Abstract

Urinary tract infections (UTIs) are a major global health concern, exacerbated by the rise of multidrug-resistant (MDR) pathogens and biofilm formation. This study evaluated the antibacterial and antibiofilm effects of green-synthesized zinc oxide nanoparticles (ZnO NPs), alone and in combination with ceftriaxone, against clinical MDR isolates of Escherichia coli and Klebsiella pneumoniae. Most isolates demonstrated biofilm-forming ability, with K. pneumoniae showing stronger biofilm production than E. coli. ZnO NPs were synthesized using Dracaena sanderiana extract and characterized by UV-Vis spectroscopy, X-ray diffraction, and TEM, confirming uniform, spherical nanoparticles with an average size of ~13 nm and hexagonal wurtzite structure. Minimum inhibitory concentration (MIC) assays revealed effective antibacterial activity, and sub-MIC treatments significantly reduced biofilm formation. Notably, combination treatment with ZnO NPs and ceftriaxone exhibited enhanced antibiofilm activity compared to individual treatments. The inhibitory effect is attributed to reactive oxygen species generation, disruption of cell membranes, and interference with biofilm matrix components. These findings suggest that ZnO NPs, particularly in combination with conventional antibiotics, represent a promising strategy to combat MDR uropathogens and improve UTI management.

Keywords:

Urinary tract infections; Multidrug-resistant bacteria (MDR); Biofilm formation; Green synthesis; Nanotechnology.

1. Introduction

Urinary tract infections (UTIs) are among the most common infectious diseases worldwide, affecting hundreds of millions of individuals annually, with over 150 million cases reported globally (Mancuso et al., 2023). They impose a significant economic burden on healthcare systems; in the United States alone, annual costs related to diagnosis, treatment, hospital admissions, and recurrent episodes exceed 3.5 billion USD (Flores-Mireles et al., 2015). In developing

countries, limited diagnostic tools, restricted antibiotic access, and the rapid spread of antimicrobial resistance further exacerbate this burden (Murray et al., 2022).

The management of UTIs is complicated by high recurrence rates and the emergence of multidrug-resistant (MDR) pathogens. Gram-negative bacteria, particularly Escherichia coli, Klebsiella pneumoniae, and Proteus mirabilis, are the primary causative agents. However, Gram-positive pathogens, notably Staphylococcus aureus, are increasingly observed in hospital-acquired UTIs, reflecting evolving epidemiology and persistent challenges in infection control (Al-Amery, 2023)

A major contributor to persistence and treatment failure is biofilm formation. Biofilms are structured communities of microorganisms embedded in a self-produced extracellular matrix, adhering to urinary catheters, epithelial surfaces, and medical devices. They protect bacteria from antibiotics and host immunity, increase tolerance, and promote chronic or recurrent infections. Biofilms also act as reservoirs for resistance genes, accelerating antimicrobial resistance dissemination (Muhammad et al., 2020).

Nanotechnology offers promising solutions against MDR pathogens. Zinc oxide nanoparticles (ZnO NPs) have broad-spectrum antibacterial activity through multiple mechanisms, including reactive oxygen species production, Zn^{2+} ion release, membrane disruption, biofilm inhibition, and quorum sensing interference, reducing bacterial virulence and persistence (Luo et al., 2024).

Despite increasing interest in the antibacterial potential of ZnO NPs, few studies have comprehensively evaluated their effects on biofilm formation. Therefore, this study aims to assess the anti-biofilm activity of green-synthesized ZnO NPs against clinical MDR isolates, providing insights for innovative therapeutic strategies to combat antimicrobial resistance and improve UTI treatment outcomes.

2. Materials and methods

2.1 Materials

Fresh leaves of D. sanderiana were obtained from a local market in Al-Anbar, Iraq. Zinc sulfate heptahydrate ($ZnSO_4 \cdot 7H_2O$, ≥ 99% purity, analytical grade) was purchased from HiMedia (India). Sodium hydroxide pellets (NaOH, ≥ 98% purity, analytical grade) were obtained from Sigma-Aldrich (USA). Blood agar, MacConkey agar, Mueller-Hinton broth (MHB), and Brain Heart Infusion broth (BHI) were acquired from HiMedia (India). Ceftriaxone (CRO, 1000 mg/vial) was procured from Acino (Switzerland). Resazurin sodium salt (≥ 90% purity) was purchased from Sigma-Aldrich (USA).

2.2 Methods

2.2.1 Collection, culturing and I dentification of clinical specimens

A total of 175 urine samples were collected from patients as mid-stream urine at AL-Ramadi Teaching Hospital for Maternity and AL-Ramadi Teaching

Hospital. Samples were cultured on blood agar and MacConkey agar and incubated at 37°C for 18–24 hours. Following bacterial growth, isolates recovered from MacConkey agar were identified and further confirmed using the VITEK 2 system with GN cards, according to the manufacturer's instructions.

2.2.2 Green biosynthesis of ZnO nanoparticles

Two grams of plant powder were placed in a 250 ml beaker, stirred, and heated at 65 ℃ in 100 ml of deionized water for a duration of 2 hours (Abo-Shama et al., 2020) .The extract was permitted to cool and subsequently centrifuged at 4000 rpm for 15 minutes, followed by filtration with Whatman filter paper No1. To synthesize ZnONPs, as illustrated in (Fig 2-1), 100 ml of 0.1 M aqueous solution of zinc sulfate was placed in a 250 ml beaker. Subsequently , 25 ml of plant extract was introduced dropwise at room temperature. The solution was stirred for 15 minutes at 65℃ and100 rpm. The pH of the solution was subsequently adjusted to 12 by dropwise addition of 2M NaOH solution. The mixture was combined and subjected to heating at 65 ℃ for a duration of 2 hours. A transition in color from pale yellow to white was observed, indicating the formation of zinc oxide nanoparticles. The resultant solution was subjected to centrifugation for 20 minutes at 4000 rpm to provide a precipitate, which was subsequently dried in an oven at 300 ℃ overnight for utilization in biological applications.

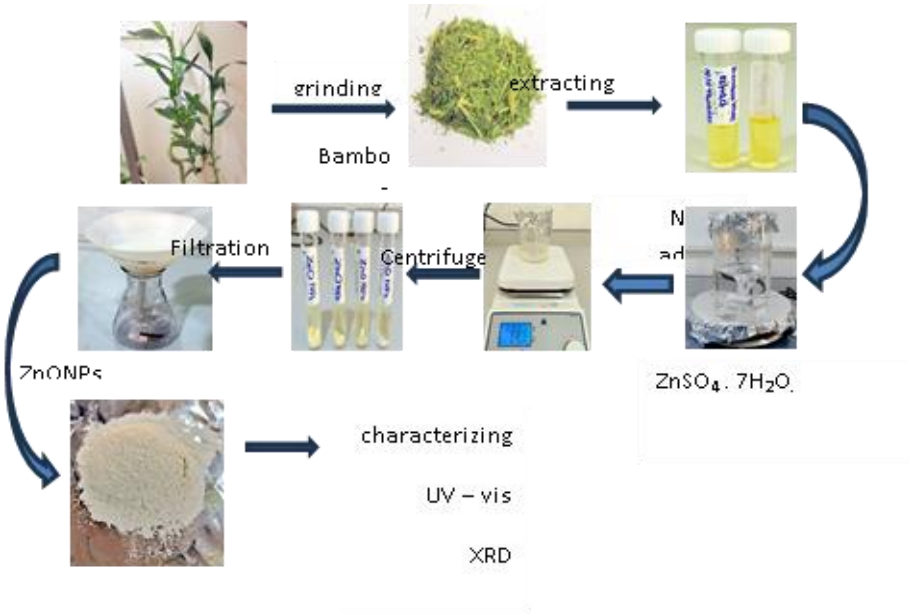

Figure (2-1): Green synthesis of ZnO NPs

2.2.3 Characterization of ZnO NPs

Characterization is essential for understanding the properties of nanoparticles. The following methods were employed to determine the characteristics of ZnO NPs. UV-visible spectroscopy was used to analyze the optical properties of the samples. X-ray diffraction (XRD) is a widely used technique in materials science for determining a material's crystallographic structure (Abbas et al., 2024). Additionally, Transmission Electron Microscopy (TEM) is used to examine the structural parameters of the nanoparticles, including size and shape. TEM analysis has revealed the morphological characteristics of green-synthesized ZnO NPs (Albarakaty et al., 2023).

2.2.4 Quantitative Assessment of Biofilm Formation

The biofilm-forming ability of E. coli and K. pneumoniae was evaluated using the methodology of Faiq and Ahmed, (2024), with slight modifications, specifically the exclusion of glucose from the BHI medium as described in the protocol. Quantitative assessment was performed using a colorimetric microtiter plate assay.

Fresh bacterial colonies were inoculated into brain heart infusion (BHI) broth, incubated, and adjusted to 0.5 McFarland turbidity. A standardized suspension (200 µL) was dispensed in triplicate into 96-well microtiter plates, with sterile BHI as a negative control. Plates were incubated aerobically at 37°C for 24 hours. Non-adherent cells were removed by washing with PBS, and biofilms were fixed with methanol, stained with crystal violet, and then solubilized with ethanol. The optical density (OD) of the stained biofilms was measured at 630 nm, and isolates were classified as non-, weak, moderate, or strong biofilm producers based on OD relative to negative control.

The biofilm-forming ability of the bacterial isolates was determined by comparing the optical density (OD) readings according to the following criteria:

$OD \leq ODc$ non-biofilm production

$ODc < OD \leq 2 \times ODc$ weak biofilm production

$2 \times ODc < OD \leq 4 \times ODc$ moderate biofilm production

$OD > 4 \times ODc$ strong biofilm production.

Where:

OD = optical density of the test isolate at 630 nm

ODc = optical density of the negative control at 630 nm

2.2.5 Determination of Minimum Inhibitory Concentration

The research employed the minimum inhibitory concentration (MIC) assay to determine the lowest concentration of ZnONPs that inhibits the growth of

MDR bacteria. A 96-well plate was filled with 100µl of Muller Hinton broth (MHB), along with serial 2-fold dilutions of ZnONPs and ceftriaxone solution. Finally, 10µl of fresh prepared bacterial culture broth. The plates were coated with self-adhesive membranes and incubated at 37°C for 24 hours. Subsequent to incubation, 20 µL of resazurin solution was added to each well. The color transitioned from blue to pink, indicating bacterial growth. The MIC was identified as the minimal concentration of ZnO NPs and CRO concentration that inhibited this color change (Hamid et al., 2024).

2.2.6 Biofilm inhibition assay

The inhibitory efficacy of ZnONPs on biofilm formation by these isolates was evaluated using the microtiter plate method as described by Jabbar et al. (2021) with some modifications to quantify the percentage of biofilm formation. The bacterial culture in brain heart infusion broth was prepared and adjusted to conform to McFarland standard No. 0.5. The suspension was subsequently inoculated with sub-MIC of ZnONPs, CRO, and their combination. In three triplicate vertical rows, 200 µl of prepared bacterial suspension containing the treatments were added to a microtiter plate for each biofilm producing bacterial isolate, while 200µl from untreated suspension was put into another three wells to serve as a control. The plate was incubated at 37 ºC for 24 hours, facilitating biofilm formation by the cells. The plate was rinsed three times with sterile distilled water and air dried at room temperature for 45 minutes. Subsequently, 200 µl of a 0.1 % crystal violet solution was added to each well for 15 minutes and rinsed again. Subsequently, 200 µL of 99 % ethanol was added to each well for 15 minutes to remove the stain from the biofilm and followed by spectrophotometer measurement.

3. Results and discussion

3.1 Isolation and Identification

A total of 175 clinical samples were analyzed, yielding 86 bacterial isolates, including 32 E. coli and 21 K. pneumoniae, along with other bacterial species. Identification using the VITEK 2 Compact system showed strong concordance with initial biochemical tests, demonstrating its reliability as a confirmatory method and its suitability as an alternative to conventional identification techniques in clinical laboratories. Previous studies, including Funke et al. (2004) and Elbehiry et al. (2016), reported accuracy rates approaching 98%, though performance may vary depending on bacterial species and card types.

3.2 Biofilm Formation

Statistical analysis demonstrated significant differences in biofilm formation intensity among weak, moderate, and strong producers within each bacterial species ($p < 0.05$). The P values for E. coli and K. pneumoniae were 0.001, indicating statistically significant variation in biofilm production levels.

Among the 32 E. coli isolates, 84.38% were weak biofilm producers, 6.25% were moderate, 6.25% were strong producers, and 3.13% were non-biofilm formers, indicating that 96.88% of the isolates were capable of forming biofilms.

In contrast, all K. pneumoniae isolates (100%) demonstrated biofilm-forming ability, with 61.90% classified as strong and 38.10% as moderate producers Table (3-1).

Table (3-1): Biofilm Formation Categories of the Studied Bacterial Isolates

Bacterial isolate	No. of isolates	Biofilm formation categories				
		Strong	Moderate	Weak	Producer	Non producer
E. coli	32	2 (6.25%)	2 (6.25%)	27 (84.38%)	31 (96.88%)	1 (3.13%)
K. pneumoniae	21	13 (61.90%)	8 (38.10%)	0%	21 (100%)	0%

These findings are consistent with previous reports indicating a higher biofilm-forming capacity in K. pneumoniae compared to E. coli, which has been attributed to the production of extracellular polysaccharides that contribute to biofilm matrix stability (Zhu et al., 2021). Variations among studies may be related to differences in environmental conditions, geographic location, study period, or the number of isolates examined.

3.3 UV-Visible Spectra of ZnO NPs

UV-Vis spectroscopy showed a characteristic absorption peak at 380 nm (Figure 3-1), confirming the formation of ZnO NPs using D. sanderiana extract. The blue shift indicates a quantum confinement effect, typical for nanoparticles smaller than the exciton Bohr radius (Kamarajan et al., 2022).

The observed peak is consistent with previous studies reporting ZnO NPs absorption between 320–390 nm (Jamdagni et al., 2018) and with other plant-mediated syntheses at ~368–370 nm (Shankar Thirumoorthy et al., 2021; Abomuti et al., 2021). Differences in some reports, such as 280 nm (Abo-Shama et al., 2020), may result from variations in extract composition, temperature, or reaction time.

These findings confirm that the synthesized ZnO NPs exhibit typical optical properties of nanoscale ZnO, validating the green synthesis method.

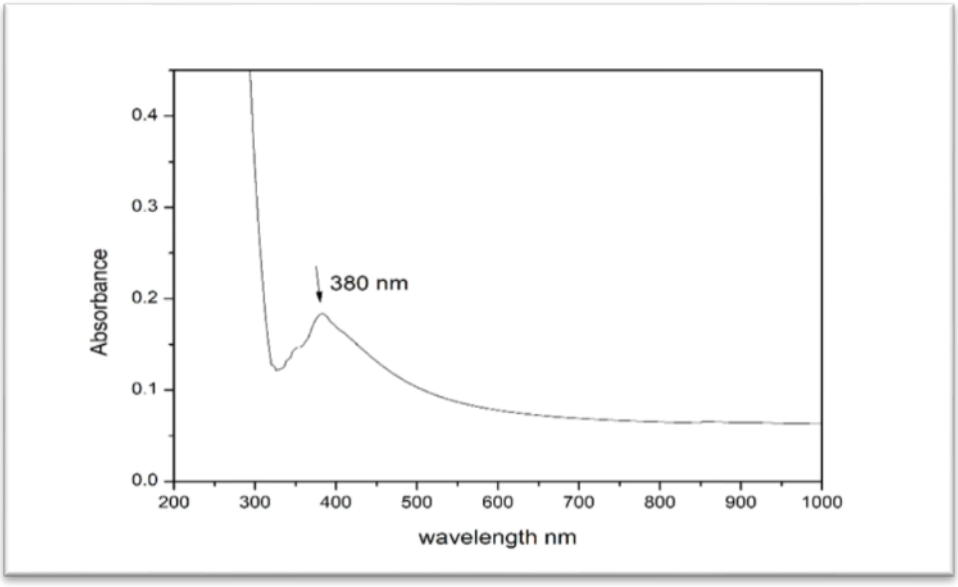

Figure (3-1): UV-Visible absorption spectrum of ZnO nanoparticles showing a characteristic absorption peak at 380 nm

3.4 X-Ray Diffraction Analysis (XRD)

The XRD pattern of the synthesized ZnO NPs exhibited characteristic peaks corresponding to the hexagonal wurtzite structure (Figure 3-2). Diffraction peaks observed at 30.1°, 33.9°, 36.6°, 44.1°, 56.6°, 60.0°, and 65.1° matched the (100), (002), (101), (102), (110), (103), and (200) planes, consistent with JCPDS card No. 36-1451. The sharp and intense peaks indicate a well-crystalline nature of the nanoparticles. The average crystallite size, calculated using Scherrer's formula, was estimated to be 41 nm, confirming the integrity of the synthesized material (Kalpana et al., 2018).

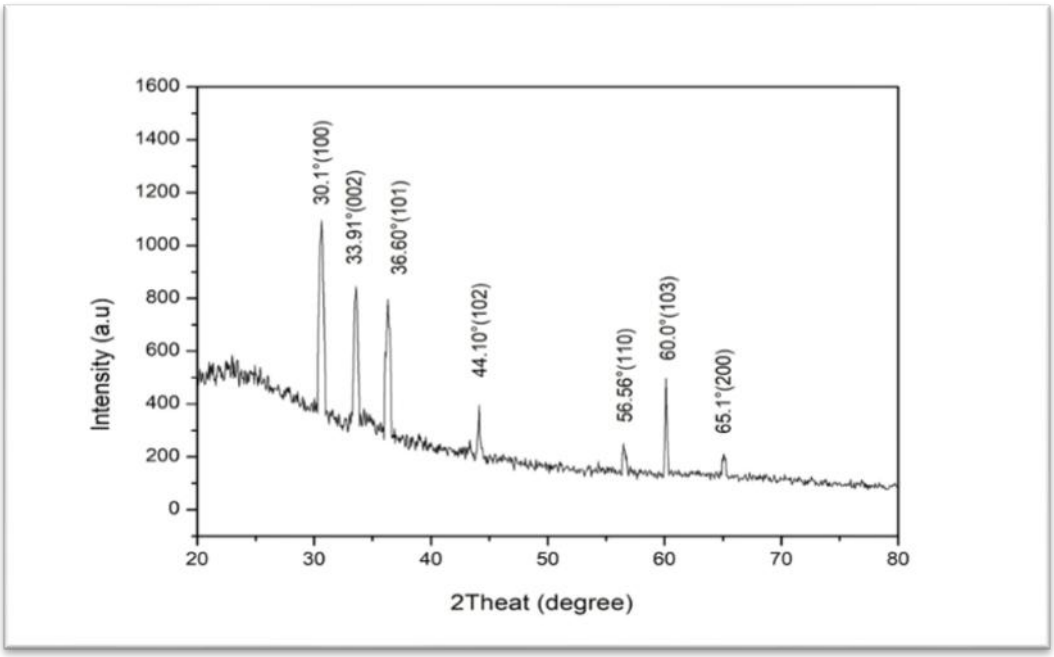

Figure (3-2): X-ray diffraction spectra of ZnONPs

These results are consistent with previous studies reporting hexagonal wurtzite ZnO NPs with distinct diffraction peaks at similar 2θ values (Abu-Muti et al., 2021; Abo-Shama et al., 2020), validating the crystalline structure achieved through the green synthesis approach.

3.5 Transmission Electron Microscopy Analysis (TEM)

TEM analysis revealed that the biosynthesized ZnO NPs exhibited a uniform spherical morphology, with particle diameters ranging from 10 to 20 nm (Figure 3-3) and an average size of approximately 13 nm. Such nanoscale dimensions are favorable for maximizing surface reactivity and enhancing interactions with bacterial cell walls.

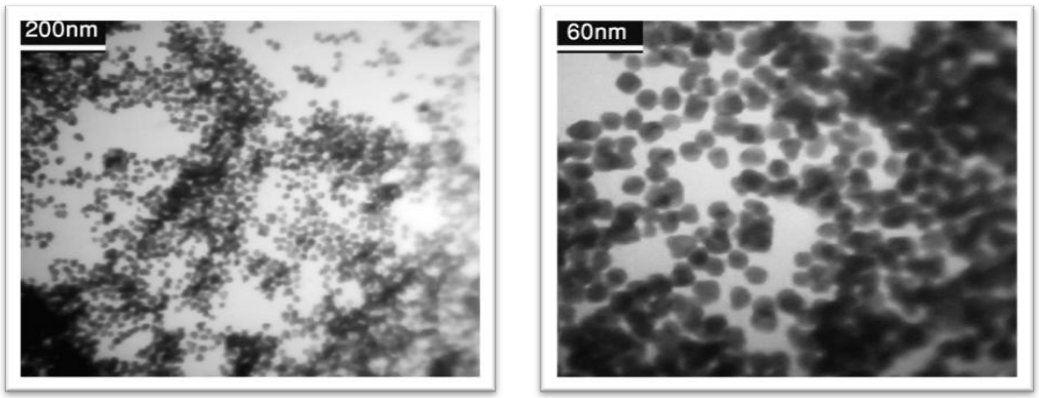

Figure (3-3): Transmission electron microscopy (TEM) images of ZnO nanoparticles.

These results are consistent with previous studies reporting comparable particle sizes (Abomuti et al., 2021), though the current NPs showed a slightly larger average size with a narrower distribution (Figure 3-4), indicating a more controlled synthesis. Variations in size and morphology among studies (Nxumalo et al., 2024; Abo-Shama et al., 2020) are likely due to differences in synthesis parameters, precursor concentration, and the nature of the biological reducing and stabilizing agents. In this study, the phytochemicals in D. sanderiana extract likely promoted uniform nucleation and growth, resulting in well-dispersed, spherical nanoparticles. Although slight agglomeration was observed, a common phenomenon due to van der Waals forces, it did not significantly affect surface reactivity or potential antibacterial activity (Shrestha et al., 2020). Overall, TEM confirms that the synthesized ZnO NPs possess a fine, uniform structure, supporting their enhanced reactivity and potential efficacy against bacterial pathogens.

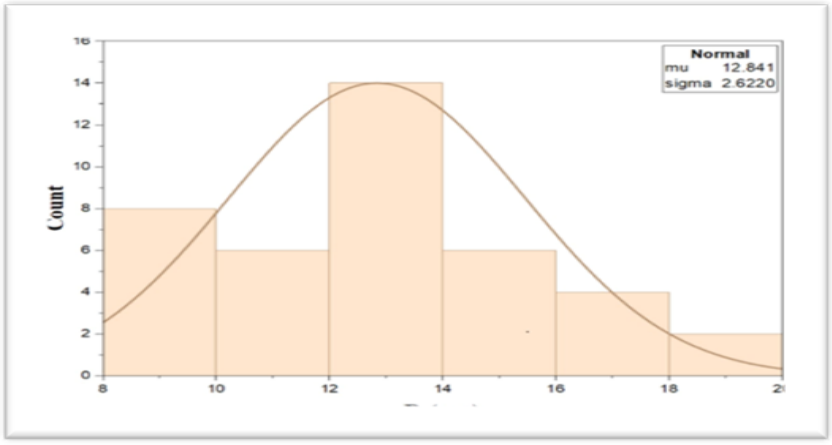

Figure (3-4): Average diameter of ZnO nanoparticles by TEM.

3.6 MIC Determination of ZnO NPs and Antibiotics Against Clinical Isolates

The experiments were conducted on multidrug-resistant (MDR) isolates, namely E. coli (E1) and K. pneumoniae (K21).The minimum inhibitory

concentration (MIC) results showed that the MIC value of ceftriaxone (CRO) was 128 µg/mL for both E. coli and K. pneumoniae. Regarding zinc oxide nanoparticles (ZnO NPs), the MIC value was 1562.5 µg/mL against E. coli and 3125 µg/mL against K. pneumoniae.

These findings demonstrate enhanced antibacterial performance against Gram-negative isolates. The antibacterial activity of ZnO NPs is generally attributed to membrane disruption, increased permeability, generation of reactive oxygen species, and the release of Zn^{2+} ions, which can damage cellular lipids, proteins, and DNA (Alshareef et al., 2021; Murali et al., 2021).

3.7 Antibiofilm Activity of ZnO NPs Against the Biofilm-producing Isolates

Biofilm formation was assessed using the crystal violet assay at 630 nm, with a negative control optical density (OD) of 0.058 as the reference value. The untreated E. coli isolate showed an OD of 0.158, indicating moderate biofilm formation. After treatment with sub-MIC concentrations of ZnO NPs (781 µg/mL) and ceftriaxone (64 µg/mL), the OD values decreased to 0.062 and 0.070, respectively. The combined treatment (195 + 16 µg/mL) further reduced the OD to 0.077, reflecting weak biofilm formation.

Similarly, the untreated K. pneumoniae isolate exhibited an OD of 0.144, indicating moderate biofilm production. Upon exposure to ZnO NPs (1562.5 µg/mL) and ceftriaxone (64 µg/mL), OD values decreased to 0.076 and 0.097, respectively. The combination treatment (390.5 + 16 µg/mL) reduced the OD to 0.096, indicating weak biofilm formation. Table (3-2).

Table (3-2): Impact of Sub-MIC Treatments on Biofilm Formation in Selected Isolates

Isolate code	OD untreated	OD (ZnO NPs at sub-MIC)	OD (Antibiotic at sub-MIC)	OD (ZnO NPs + antibiotic at sub-MIC)
E1	0.158	0.062	0.070	0.077
K21	0.144	0.076	0.097	0.096

The inhibitory effect of ZnO NPs on biofilm formation can be attributed to multiple complementary mechanisms. Primarily, ZnO NPs generate ROS, leading to damage of the bacterial cell membrane and destabilization of the biofilm. In parallel, they reduce bacterial cell surface hydrophobicity, thereby weakening bacterial adhesion and aggregation, as demonstrated by Abdelghafar et al. (2022).

Nanoparticles can also act at multiple levels by targeting key bacterial components involved in biofilm development and maintenance. These include extracellular DNA (eDNA), which plays a critical role in bacterial adhesion, aggregation, biofilm formation, structural integrity, and intercellular communication (Abadeer et al., 2015).

Overall, the treatments significantly reduced biofilm formation in both isolates, demonstrating the antibiofilm potential of ZnO NPs alone and in

combination with antibiotics.

The differences between study results may be attributed to variations in bacterial isolate types, nanoparticle concentrations, the type of antibiotic used, and biofilm incubation conditions such as temperature, incubation time, and culture medium. Additionally, the physicochemical properties of the nanoparticles, including size, shape, and surface charge, can influence inhibitory efficacy, explaining the variability observed among different studies.

References:

Mancuso, G., Midiri, A., Gerace, E., Marra, M., Zummo, S., & Biondo, C. (2023). Urinary Tract Infections: The Current Scenario and Future Prospects. In Pathogens (Vol. 12, Issue 4). MDPI. https://doi.org/10.3390/pathogens12040623

Flores-Mireles, A. L., Walker, J. N., Caparon, M., & Hultgren, S. J. (2015). Urinary tract infections: Epidemiology, mechanisms of infection and treatment options. In Nature Reviews Microbiology (Vol. 13, Issue 5). https://doi.org/10.1038/nrmicro3432

Murray, C. J., Ikuta, K. S., Sharara, F., Swetschinski, L., Robles Aguilar, G., Gray, A., Han, C., Bisignano, C., Rao, P., Wool, E., Johnson, S. C., Browne, A. J., Chipeta, M. G., Fell, F., Hackett, S., Haines-Woodhouse, G., Kashef Hamadani, B. H., Kumaran, E. A. P., McManigal, B., … Naghavi, M. (2022). Global burden of bacterial antimicrobial resistance in 2019: a systematic analysis. The Lancet, 399(10325). https://doi.org/10.1016/S0140- 6736(21)02724-0

Al-Amery, A. N. H. (2023). Bacteriological study of Urinary Tract Infection Associated with Urinary Catheterization in Hospitals [Master's thesis]. University of Tikrit

Muhammad, M. H., Idris, A. L., Fan, X., Guo, Y., Yu, Y., Jin, X., Qiu, J., Guan, X., & Huang, T. (2020). Beyond Risk: Bacterial Biofilms and Their Regulating Approaches. In Frontiers in Microbiology (Vol. 11). Frontiers Media S.A. https://doi.org/10.3389/fmicb.2020.00928

Luo, L., Huang, W., Zhang, J., Yu, Y., & Sun, T. (2024). Metal-Based Nanoparticles as Antimicrobial Agents: A Review. ACS Applied Nano Materials, 7(3), 2529– 2545. https://doi.org/10.1021/acsanm.3c05615

Abomuti, M. A., Danish, E. Y., Firoz, A., Hasan, N., & Malik, M. A. (2021). Green Synthesis of Zinc Oxide Nanoparticles Using Salvia officinalis Leaf Extract and Their Photocatalytic and Antifungal Activities. Biology, 10(11), 1075. https://doi.org/10.3390/biology10111075

Abo-Shama, U. H., El-Gendy, H., Mousa, W. S., Hamouda, R. A., Yousuf, W. E., Hetta, H. F., & Abdeen, E. E. (2020). Synergistic and antagonistic effects of metal nanoparticles in combination with antibiotics against some reference strains of pathogenic microorganisms. Infection and Drug Resistance, 13, 351–362. https://doi.org/10.2147/IDR.S234425

Albarakaty, F. M., Alzaban, M. I., Alharbi, N. K., Bagrwan, F. S., Abd El-Aziz, A. R. M., & Mahmoud, M. A. (2023). Zinc oxide Nanoparticles,

Biosynthesis, characterization and their potent photocatalytic degradation, and antioxidant activities. Journal of King Saud University - Science, 35(1), 102434. https://doi.org/10.1016/j.jksus.2022.102434

Faiq, N. H., & Ahmed, M. E. (2024). Effect of Biosynthesized Zinc oxide Nanoparticles on Phenotypic and Genotypic Biofilm Formation of Proteus mirabilis. Baghdad Science Journal, 21(3), 894–908. https://doi.org/10.21123/bsj.2023.8067

Hamid, L. L., Hassan, M. H., & Obaid, A. S. (2024). Allium sativum extract mediate

154 the biosynthesis of palladium nanoparticles as potential nanodrug for combating multidrug-resistant bacteria and wound healing. Materials Chemistry and Physics, 321. https://doi.org/10.1016/j.matchemphys.2024.129507

Jabbar, R. N., Turki, A. M., Jamal, M., Al-Taee, M., Al-Ethawi, A. M. T., & Jabbar Al-Gafari, R. N. (2021). THE EFFECT OF GOLD NANOPARTICLES IN GROWTH AND BIOFILM FORMATION OF METHECILLIN RESISTANT STAPHYLOCOCCUS AUREUS MRSA ISOLATED FROM VARIOUS CLINICAL CASES. https://www.researchgate.net/publication/353331792

Abbas, H. M., Al Marjani, M. F., & Gdoura, R. (2024). Evaluation of the antibacterial activity of CuO and ZnO nanoparticles against uropathogenic Escherichia coli. Journal of Taibah University for Science, 18(1). https://doi.org/10.1080/16583655.2024.2322776

Elbehiry, A., Al-Dubaib, M., Marzouk, E., Osman, S., & Edrees, H. (2016). Performance of <scp>MALDI</scp> biotyper compared with Vitek TM 2 compact system for fast identification and discrimination of Staphylococcus species isolated from bovine mastitis. MicrobiologyOpen, 5(6), 1061–1070. https://doi.org/10.1002/mbo3.389

Funke, G., & Funke-Kissling, P. (2004). Evaluation of the New VITEK 2 Card for Identification of Clinically Relevant Gram-Negative Rods. Journal of Clinical Microbiology, 42(9), 4067–4071. https://doi.org/10.1128/JCM.42.9.4067-4071.2004

Zhu, J., Wang, T., Chen, L., & Du, H. (2021). Virulence Factors in Hypervirulent Klebsiella pneumoniae. In Frontiers in Microbiology (Vol. 12). Frontiers Media S.A. https://doi.org/10.3389/fmicb.2021.642484

Kamarajan, G., Anburaj, D. B., Porkalai, V., Muthuvel, A., & Nedunchezhian, G. (2022). Green synthesis of ZnO nanoparticles using Acalypha indica leaf extract and their photocatalyst degradation and antibacterial activity. Journal of the Indian Chemical Society, 99(10), 100695. https://doi.org/10.1016/j.jics.2022.100695

Jamdagni, P., Khatri, P., & Rana, J. S. (2018). Green synthesis of zinc oxide nanoparticles using flower extract of Nyctanthes arbor-tristis and their antifungal activity. Journal of King Saud University - Science, 30(2), 168–175. https://doi.org/10.1016/j.jksus.2016.10.002

Shankar Thirumoorthy, G., Balasubramaniam, O., Kumaresan, P., Muthusamy, P., &

Subramani, K. (2021). Tetraselmis indica Mediated Green Synthesis of Zinc Oxide (ZnO) Nanoparticles and Evaluating Its Antibacterial, Antioxidant, and Hemolytic Activity. https://doi.org/10.1007/s12668-020-00817-y/Published

Kalpana, V. N., Kataru, B. A. S., Sravani, N., Vigneshwari, T., Panneerselvam, A., & Devi Rajeswari, V. (2018). Biosynthesis of zinc oxide nanoparticles using culture filtrates of Aspergillus niger: Antimicrobial textiles and dye degradation studies. OpenNano, 3. https://doi.org/10.1016/j.onano.2018.06.001

Nxumalo, K. A., Adeyemi, J. O., Leta, T. B., Pfukwa, T. M., Okafor, S. N., & Fawole, O. A. (2024). Antifungal properties and molecular docking of ZnO NPs mediated using medicinal plant extracts. Scientific Reports, 14(1). https://doi.org/10.1038/s41598-024-68979-3

Shrestha, S., Wang, B., & Dutta, P. (2020). Nanoparticle processing: Understanding and controlling aggregation. Advances in Colloid and Interface Science, 279, 102162. https://doi.org/10.1016/j.cis.2020.102162

Murali, M., Kalegowda, N., Gowtham, H. G., Ansari, M. A., Alomary, M. N., Alghamdi, S., Shilpa, N., Singh, S. B., Thriveni, M. C., Aiyaz, M., Angaswamy, N., Lakshmidevi, N., Adil, S. F., Hatshan, M. R., & Amruthesh, K. N. (2021). Plant-mediated zinc oxide nanoparticles: Advances in the new millennium towards understanding their therapeutic role in biomedical applications. Pharmaceutics, 13(10). https://doi.org/10.3390/pharmaceutics13101662

Alshareef, F. O., Alkoblan, D. K., Mateen, A., & Albarag, A. M. (2021). Synergistic effects of zinc oxide nanoparticles and various antibiotics combination against Pseudomonas aeruginosa clinically isolated bacterial strains. Saudi Journal of Biological Sciences, 28(1), 928–935. https://doi.org/10.1016/j.sjbs.2020.09.064

Abdelghafar, A., Yousef, N., & Askoura, M. (2022). Zinc oxide nanoparticles reduce biofilm formation, synergize antibiotics action and attenuate Staphylococcus aureus virulence in host; an important message to clinicians. 141

BMC Microbiology, 22(1). https://doi.org/10.1186/s12866-022-02658-z

Abadeer, N. S., Fülöp, G., Chen, S., Käll, M., & Murphy, C. J. (2015). Interactions of Bacterial Lipopolysaccharides with Gold Nanorod Surfaces Investigated by Refractometric Sensing. ACS Applied Materials & Interfaces, 7(44), 24915–24925. https://doi.org/10.1021/acsami.5b08440